detection procedure was performed as described previously (Saito et al. 2005).

RNA preparation and reverse transcription/PCR

Total RNA was isolated from primary PDL cells (both from healthy volunteer B and the MFS1 patient) and from immortalized PDL cells cultured in α–MEM containing 10% FBS, by using ISOGEN (Nippon Gene, Japan) according to the manufacturer's instructions. cDNA was synthesized from 1 μg total RNA by QuantiTect Reverse Transcription (QIAGEN, Germany), and each cDNA was used as the template for subsequent PCR amplification. Amplification was performed in a GeneAmp PCR System 9700 (Applied Biosystems). The reaction conditions were 94°C for 1 min, 60°C for 30 s, and 72°C for 30 s. The sequences of the used primers were: *POSTN* encoding periostin, sense 5′-ATTGATGGAGTGCCTGTG-3′, antisense 5′-CCTTGGTGACCTCTTCTTG-3′; *ASPN* encoding asporin, sense 5′-CGATACAAAGAACTACAAAGGCT GG-3′, antisense 5′-GCATTTCCCAGTATTTCA CCG-3′; *COL12A1* encoding collagen type XII, sense 5′-CGGA CAGAGCCTTA CGTGCC-3′, antisense 5′-CTGCCC GGGTCCGTGG-3′; *BGLAP* encoding osteoclacin, sense 5′-CCTTTGTGTCCAAGCAGGAG-3′, antisense 5′-TCA GCCAACTCGTCACAGTC-3′; *OPN* encoding osteopontin, sense 5′-TTGCAGTGATTTGCTTTTGC-3′, antisense 5′-TGTGGGG CTAGGAGATTCTG-3′; *BSP* encoding bone sialoprotein, sense, 5′-GAACCACTTCCCCACCT TTT-3′, antisense 5′-TCTGACCATCATAGCCATCG-3′; *COL1A1* encoding collagen type I, sense 5′-CTGACCTT CCTGCGCCTGATGTCC-3′, antisense 5′-GTCTGGGGC ACCAACGTCCAAGGG -3′; and a human gene encoding β-actin, sense 5′-ATGAGGATCCTCACCGAGCGCGGCT ACAG C-3′, antisense 5′-ACACCACTGTGTTGGCGTAC AGGTCTTTGC-3′. Optimization of PCR cycle number to allow semi-quantitative analysis was performed by generating saturation curves of amplified product against cycle number. Saturation was seen with 33, 34, 31, 34, 41, 41, 25, and 25 cycles for *POSTN*, *ASPN*, *COL12A1*, *BGLAP*, *OPN*, *BSP*, *COL1A*, and β-actin, respectively. Thus, the semi-quantitative gene expression analysis by reverse transcription/PCR (RT-PCR) was performed with 30, 31, 28, 31, 39, 39, 23, and 23 cycles for *POSTN*, *ASPN*, *COL12A1*, *BGLAP*, *OPN*, *BSP*, *COL1A*, and β-actin, respectively.

A 151-bp fragment of *POSTN* (2220–2370 in NM_006475), a 292-bp fragment of *ASPN* (1031–1322 in NM_017680) (Yamada et al. 2001), a 180-bp fragment of *COL12A1* (7041–7220 in NM_080645), a 151-bp fragment of *BGLAP* (122–272 in NM_199173), a 166-bp fragment of *OPN* (173–338 in NM_001040058), a 201-bp fragment of *BSP* (876–1076 in NM_004967), a 300-bp fragment of *COL1A1* (4180–4479 in NM_000088), and a 327-bp fragment of the gene encoding β-actin (641–967 in NM_001101) were separated on 2% agarose gels (Nippon Gene, Japan) by electrophoresis. The gels were stained with ethidium bromide, photographed under ultraviolet excitation, and analyzed by using picture-imaging software (Scion Image, Scion, Md.).

Cell adhesion assay

To examine the adhesion of PDL cells, viz., HPDL2 from healthy volunteer 2 and M-HPL1 from the MFS1 patient, to hydroxyapatite particles (size 300–500 μm; OSferion, Olympus, Japan), both types of cells were labeled by using the PKH26 Red Fluorescent Cell Linker Mini Kit (Sigma) and incubated with hydroxyapatite particles for 18 h in α–MEM containing 10% FBS. The attached cells were observed by using a fluorescence microscope (AF6000, Leica, Germany).

In vivo differentiation assay

Fiber formation in the HPDL2 and M-HPL1 cells was assessed as described previously (Handa et al. 2002; Saito et al. 2005; Yokoi et al. 2007). Briefly, 1.5×10^6 cells were incubated with 40 mg hydroxyapatite particles and fibrin clot (mixture of mouse fibrinogen and thrombin; Sigma). They were transplanted subcutaneously into 5-week-old male CB-17 *SCID/SCID* mice (Nihon Crea, Japan). Mice were sacrificed after 4 weeks and implanted tissues were collected. Three transplants were prepared for each group, and experiments were repeated in triplicate.

To examine human (not mouse) vimentin-positive cells in transplanted tissues, tissues were fixed in 4% PFA for 1 day, decalcified with 10% formic acid for 3 days, and embedded in paraffin, and 5-μm-thick sections were prepared. To avoid non-specific staining by mouse monoclonal antibodies, sections were blocked by using the M.O.M. kit (Vector Laboratories, Calif.) as previously described (Handa et al. 2002). Sections were incubated, for 1 h, with anti-human vimentin monoclonal antibody (V9, DAKO, Calif.), which recognizes human but not mouse cells. After being washed, sections were incubated with biotinylated secondary antibody (M.O.M. kit) and avidin-peroxidase conjugate (M.O.M. kit). The reaction was visualized by using diaminobenzidine.

To examine human fibrillin-1-positive cells, transplanted tissues were embedded in carboxymethyl cellulose compound (Finetec, Japan), and 5-μm-thick frozen sections were prepared (Kawamoto and Shimizu 2000). Frozen sections were incubated with anti-human fibrillin-1 rabbit polyclonal antibody (Elastin Products, Mo.) for 1 h. After being washed, sections were incubated with Alexa Fluor 594 goat anti-rabbit IG (H+L; Invitrogen), and fluorescence

was observed with a fluorescence microscope (AF6000, Leica, Germany).

Statistical analysis

Student's *t*-test was used to analyze differences in cell numbers between M-HPL1 and HPDL2. Each difference was considered significant at a *P*-value of less than 0.05.

Results

MFS1 patient with a heterozygous mutation in cbEGF domain of FBN1

As shown in Fig. 1a–d, the 46-year-old female patient had severe periodontitis. All teeth had to be extracted before the surgical replacement of the mitral valve to avoid infective endocarditis. Mutational analysis of *FBN1* and *TGFBR2* was performed by using a genomic DNA sample. Since *FBN1* and *TGFBR2* have 65 and 7 exons, respectively, screening of gene mutations before direct sequencing was performed by DHPLC. In total, 65 and 8 amplicons of *FBN1* and *TGFBR2*, respectively, were amplified by PCR and subsequently analyzed by DHPLC. Among them, the peak in the amplicon of exon 52 in *FBN1* from the MFS1 patient shifted to the left compared with that of the wild-type sample (Fig. 1e). This demonstrated heteroduplex formation of the amplicon from the MFS1 patient. Direct sequencing of this product was performed (Fig. 1f). A heterozygous mutation (A to G) was seen at position 6431 (from the translation site in NM_000138). This missense mutation resulted in the replacement of Asn by Ser at amino acid position 2144 (N2144S) in the 32th cbEGF domain (Fig. 1g; see also in previous study of this MFS1 patient in Hewett et al. 1993). Thus, this is not a single nucleotide polymorphism (SNP) or a novel mutation. The elution profile of DHPLC for *TGFBR2* did not show differences between the wild-type sample and MFS1 patient.

Phenotype of primary PDL cells with N2144S mutation from MFS1 patient

Cells were isolated from the PDL of extracted teeth from the MFS1 patient and were cultured in vitro. In order to examine the cellular phenotype of these isolated PDL cells, ALP activity (Fig. 2a) and mineralization (Fig. 2b) were examined. In the cell differentiation medium containing

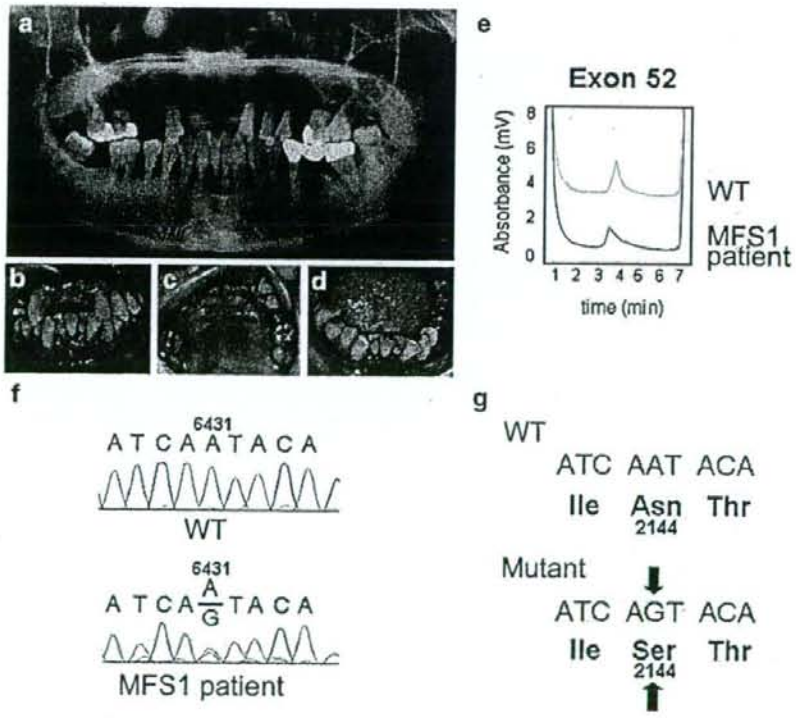

Fig. 1 Severe periodontitis and mutational analysis of the MFS1 patient. **a** In the panoramic X-ray, severe alveolar bone loss was observed around tooth roots. **b–d** Oral photographs showing the severe periodontitis of the patient. **e** DHPLC analysis of exon 52 in *FBN1*. Note the peak in the elution profile of the MFS1 patient shifted to the left compared with that of the wild-type (WT), demonstrating heteroduplex formation. **f** Nucleotide sequence of exon 52 in *FBN1*. **g** Amino acid sequence of fibrillin-1. The 6431A→G change resulted in the heterozygous missense mutation of Asn to Ser (N2144S)

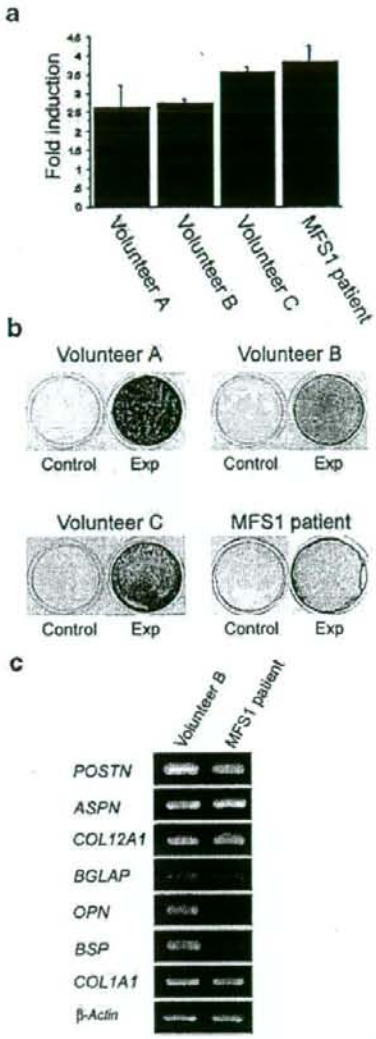

Fig. 2 **a** ALP activities of primary PDL cells isolated from three healthy volunteers (*volunteers A–C*) and the *MFS1 patient*. PDL cells were cultured in the cell differentiation medium containing ascorbic acid (50 μg/ml), β-glycerophosphate (10 mM), and dexamethasone (10 nM) for 3 weeks. Each ALP activity is represented as the ratio (*Fold induction*) to the value before culturing in the cell differentiation medium. PDL cells isolated from the MFS1 patient showed increased ALP activity as in healthy volunteers. **b** Mineralization of PDL cells cultured in the cell differentiation medium for 3 weeks. All PDL cells cultured in the cell differentiation medium were stained positively with Alizarin Red (*Exp*), but were negative when cultured in the medium containing 10% FBS solely (*Control*). **c** Expression of PDL-related genes, such as *POSTN* encoding periostin, *ASPN* encoding asporin, *COL12A1* encoding collagen type XII, *BGLAP* encoding osteocalcin, *OPN* encoding osteopontin, *BSP* encoding bone sialoprotein, *COL1A1* encoding collagen type I, and a human gene encoding β-actin, in cells from volunteer B and the MFS1 patient; reverse transcription/polymerase chain reaction (RT-PCR)

β-glycerophosphate, dexamethasone and ascorbic acid, these cells showed increased ALP activity, as did PDL cells of healthy volunteers (volunteers A–C) after a 3-week culture (Fig. 2a). The PDL cells from the MFS1 patient and healthy volunteers showed mineralization in the cell differentiation medium, but not in the medium only containing 10% FBS (Fig. 2b). The levels of the mineralization varied among cultures. Based on the similarities in the level of mineralization, PDL cells from volunteer B and MFS1 patient were selected for use in the further experiments.

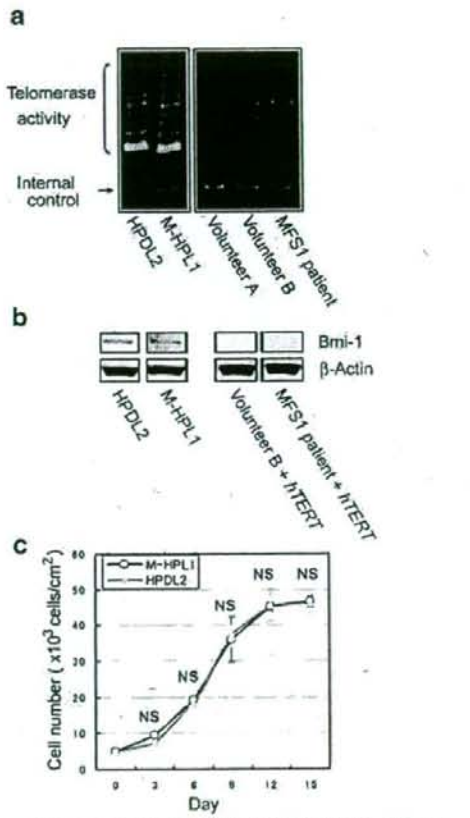

Fig. 3 **a, b** Telomerase activity and Western blot analysis of Bmi-1, respectively, in *hTERT*- and *Bmi-1*-transfected HPDL2 (originally from healthy volunteer B) and M-HPL1 (originally from the MFS1 patient). Note the characteristic ladder formation showing telomerase activity in HPDL2 and M-HPL1, but not in untransfected cells (volunteers A or B or MFS1 patient). Western blot analysis showing the expression of Bmi-1 in HPDL2 and M-HPL1, but not in cells transfected solely with *hTERT* (*Volunteer B + hTERT, MFS1 patient + hTERT*). **c** Proliferation of HPDL2 and M-HPL1 in culture. No significant difference occurs in the growth of the two types of cells at days 3, 6, 9, 12, 15 (*NS* not significant). Data represent means ± SD (n=3)

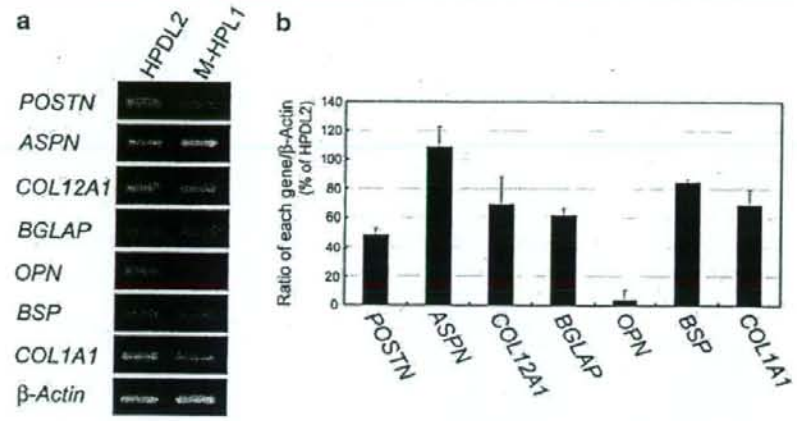

Fig. 4 **a** Expression of *POSTN* encoding periostin, *ASPN* encoding asporin, *COL12A1* encoding collagen type XII, *BGLAP* encoding osteocalcin, *OPN* encoding osteopontin, *BSP* encoding bone sialoprotein, *COL1A1* encoding collagen type I, and a human gene encoding β-actin in immortalized HPDL2 and M-HPL1; RT-PCR. **b** Densitometric data were normalized to β-actin in both types of cells. The bar graph represents the ratios of the expression of each gene in M-HPL1 (% of HPDL2). Data represent means ± SD (n=3)

The expression of various PDL-related genes was examined in cells from volunteer B and MFS1 patient by RT-PCR (Fig. 2c). Both types of PDL cells expressed *POSTN*, *ASPN*, *COL12A1*, *BGLAP*, *BSP*, and *COL1A1*. PDL cells from volunteer B expressed *OPN*. These results demonstrated that, induced by the culture conditions, the isolated PDL cells could differentiate into an osteoblastic phenotype.

Immortalization of isolated PDL cells

Since human cells have a limited life span (Sherr and DePinho 2000), and since the present PDL cells from the MFS1 patient with N2144S are valuable from a research viewpoint, the cultured cells (primary cells from volunteer B and MFS1 patient) were immortalized by retrovirus-mediated transduction. Non-transduced PDL cells and PDL cells transduced solely with *hTERT* showed senescence by passage 15. In contrast, PDL cells transduced with *Bmi-1* and *hTERT* did not show cellular senescence up to passage 20 as indicated by their cell morphology. Thus, we decided to transduce cells with both *Bmi-1* and *hTERT*. The transduced PDL cells from healthy volunteer B and the MFS1 patient were termed HPDL2 and M-HPL1, respectively.

Activation of telomerase by the transduction of *hTERT* was confirmed by the telomerase repeat amplification assay (Fig. 3a). Overexpression of Bmi-1 was confirmed by Western blot analysis (Fig. 3b). Bmi-1 was easily detected in M-HPL1 and HPDL2, but not in cells transduced solely with *hTERT*. No significant difference was seen in the cell growth between HPDL2 and M-HPL1 cultured in medium with 10% FBS up to day 15 (Fig. 3c). After day 12, the cell numbers of neither HPDL2 nor M-HPL1 increased extensively, suggesting that both types of cells had limited proliferation.

Phenotype of HPDL2 and M-HPL1

To characterize the phenotype of the immortalized PDL cells, expression of the reported PDL-related genes and β-actin was examined by semi-quantitative RT-PCR (Fig. 4a). HPDL2 and M-HPL1 both expressed *POSTN*, *ASPN*, *COL12A1*, *BGLAP*, *BSP*, and *COL1A1*. The relative expression of *POSTN*, *COL12A1*, *BGLAP*, and *COL1A1* was lower in M-HPL1 than in HPDL2 (Fig. 4b). *OPN* was expressed in HPDL2, but this was scarcely expressed in M-HPL1 (Fig. 4a, b). Immunohistochemistry with antibodies

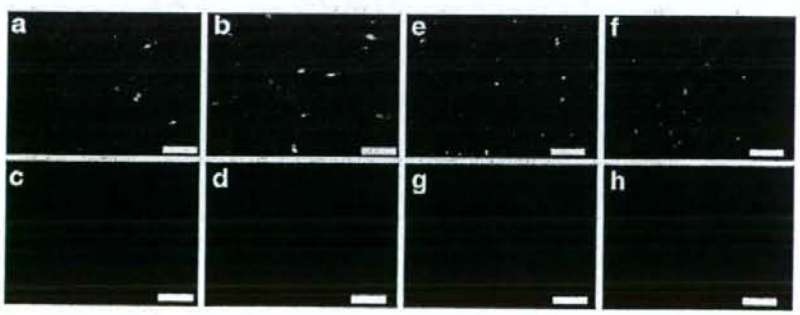

Fig. 5 Positive immunohistochemical localization of collagen type XII in cultured HPDL2 (**a**) and M-HPL1 (**b**) and of periostin in cultured HPDL2 (**e**) and M-HPL1 (**f**). Primary antibodies were replaced with mouse IgG (**c** HPDL2, **d** M-HPL1) or normal rabbit serum (**g** HPDL2, **h** M-HPL1) for negative controls. *Bars* 100 μm

against collagen type XII (Fig. 5a, b) and periostin (Fig. 5e, f) showed numerous immunostained cells in cultures of HPDL2 and M-HDL1. Staining was scarcely seen in negative controls in which primary antibodies had been replaced with mouse IgG (Fig. 5c, d) or normal rabbit serum (Fig. 5g, h).

In the lung (Neptune et al. 2003) and cardiovascular (Ng et al. 2004) systems, gene mutation in *FBN1* has been suggested to be involved in the activation of TGF-β. To examine whether this is the case in M-HPL1, immunostaining with LC1-30, which only recognizes the active form of TGF-β, was performed. M-HPL1 showed more intense staining than HPDL2 (Fig. 6e, f), although a comparable reaction was seen in HPDL2 and M-HPL1 to the antibody against LAP-β1, which also forms complexes with TGF-β (Fig. 6a, b; Miyazono et al. 1993). Staining was scarcely seen in negative controls, in which primary antibodies were replaced with normal goat serum (Fig. 6c, d) or normal rabbit serum (Fig. 6g, h).

Cell and fiber alignments in tissues transplanted with M-HPL1

Ectopic fiber formation by M-HPL1 and HPDL2 in the subcutaneous tissues of SCID mice was examined by transplantation of these cells with hydroxyapatite particles. In this experiment, hydroxyapatite was chosen because it is the major inorganic component of teeth and bones (Ten Cate 1998). HPDL2 (Fig. 7a) and M-HPL1 (Fig. 7b) both attached to the hydroxyapatite particles 18 h after being mixed with the particles.

Four weeks after the transplantation of the cells with hydroxyapatite particles into SCID mice, sections of the cells were immunostained with anti-vimentin antibody recognizing only human but not mouse cells. HPDL2 aligned in parallel between the particles (Fig. 8a, c). In contrast, M-HDL1 were

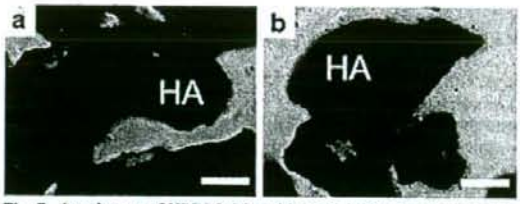

Fig. 7 Attachment of HPDL2 (**a**) and M-HPL1 (**b**) to hydroxyapatite particles (*HA*) after 18-h culture. *Bars* 100 μm

mainly located around the particles and were aligned irregularly (Fig. 8b, d). Similar observations were also seen in eight other transplants from a total of three SCID mice.

Transplanted tissues were immunostained with anti-human fibrillin-1 antibody. In contrast to the elaborate network of immunoreactive fibrillin-1 in HPDL2, M-HPL1 showed disorganized microfibril assembly (Fig. 9a, b). Staining was scarcely seen in the tissues in which the hydroxyapatite particles without cells were transplanted into SCID mice (Fig. 9c), demonstrating that the antibody only recognized human cells but not mouse cells.

Discussion

The present Japanese female patient had profound skeletal and cardiovascular symptoms including tall stature, arachnodactyly, aortic dissection, mitral valve prolapse, and severe periodontitis. Two types of Marfan syndrome (type I, MIM #154700; type II, MIM #154705) have been described so far. A large French family has been reported to exhibit the skeletal and cardiovascular features of Marfan syndrome in an autosomal dominant manner (Boileau et al. 1993). No mutation in *FBN1* has been seen in this family, and they have been classified as MFS2. Recently, *TGFBR2*

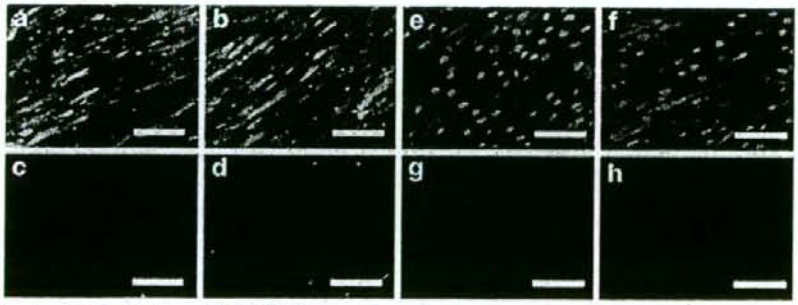

Fig. 6 Immunohistochemical localization of LAP-β1 in cultured HPDL2 (**a**) and M-HPL1 (**b**) and of LCI-30 in cultured HPDL2 (**e**) and M-HPL1 (**f**). Note that LCI-30, which recognizes only the active form of TGF-β, immunoreacts more abundantly in M-HPL1 than in HPDL2, whereas the level of LAP-β1 was comparable in the both types of cells. Primary antibodies were replaced with normal goat serum (**c** HPDL2, **d** M-HPL1) or normal rabbit serum (**g** HPDL2, **h** M-HPL1) for negative controls. *Bars* 100 μm

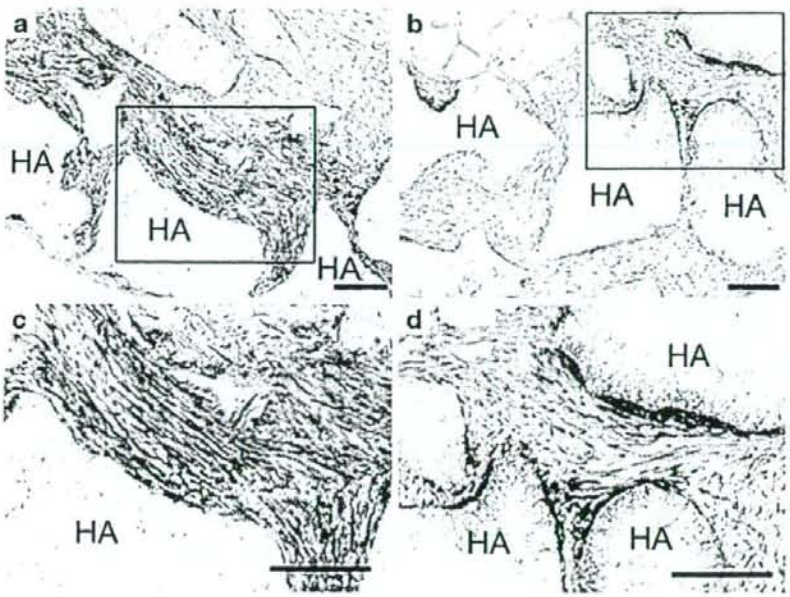

Fig. 8 Sections prepared from tissues in which HPDL2 (**a**, **c**) or M-HPL1 (**b**, **d**) were transplanted with hydroxyapatite particles (*HA*) into SCID mice for 4 weeks. Immunostaining with anti-human vimentin monoclonal antibody. The *boxed areas* in **a**, **b** are shown at higher magnification in **c**, **d**, respectively. Note that HPDL2 aligned in an organized manner, but M-HPL1 showed disorganized alignment. *Bars* 100 μm

has been identified as the responsible gene in MFS2 (Mizuguchi et al. 2004). The present patient has a heterozygous mutation in *FBN1* (Fig. 1f); this mutation results in a missense substitution (N2144S; Fig. 1g), clearly identifying the disease as MFS1.

Since *FBN1* is a large gene with 65 exons, direct sequencing of all the exons to identify mutations is time-consuming and costly. Therefore, we have performed DHPLC to screen for mutations in *FBN1*. In total, 65 amplicons for *FBN1* and 8 amplicons for *TGFBR2* have been synthesized by using specific primers by PCR. Heteroduplex formation has been identified in the product of exon 52 in *FBN1* by DHPLC (Fig. 1e). By using this method, systems have previously been developed to screen 20 congenital disorders (Kosaki et al. 2005). The present DHPLC method is a sensitive and powerful tool that allows the screening of gene mutations before direct sequencing; this is especially useful for large genes such as *FBN1*.

Cells isolated from the PDL of our MFS1 patient and of healthy volunteers have both shown increased ALP activity and mineralization in the cell differentiation medium. PDL cells are known to show an osteoblastic phenotype when cultured under these conditions (Cho et al. 1992; Giannopoulou and Cimasoni 1996; Nohutcu et al. 1997; Chien et al. 1999). After immortalization of cells by introducing *hTERT* and *Bmi-1*, both HPDL2 and M-HPL1 express PDL-related genes, viz., *POSTN* (Fujii et al. 2006), *ASPN* (Yamada et al. 2001), *COL12A1* (Fujii et al. 2006), *BGLAP* (Fujii et al. 2006), *BSP* (Yokoi et al. 2007), and *COL1A1* (Yokoi et al. 2007; Fig. 4a). These observations demonstrate that both types of cells have the characteristic phenotype of cultured PDL cells. However, *POSTN*, *COL12A1*, *BGLAP*, and *COL1A1*

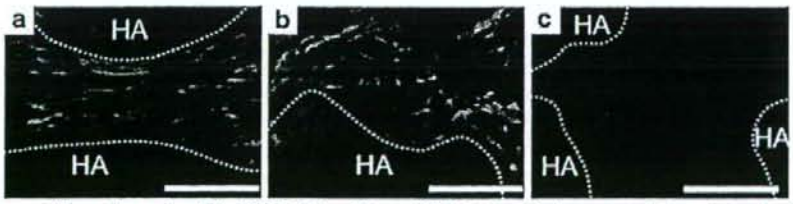

Fig. 9 Sections prepared from tissues in which HPDL2 (**a**) or M-HPL1 (**b**) were transplanted with hydroxyapatite particles (*HA*) into SCID mice for 4 weeks (*dotted lines* outline of HA). Immunostaining with anti-human fibrillin-1 antibody. Note the irregular microfibril assembly in the tissue implanted with M-HPL1 (**b**) but not in that with HPDL2 (**a**). **c** Sections prepared from tissues in which HA particles without cells were transplanted into SCID mice for 4 weeks. Note the absence of immunostaining with anti-human fibrillin-1 antibody (*dotted lines* outline of HA). *Bars* 50 μm

exhibit a lower expression in M-HPL1 than in HPDL2, and *OPN* is hardly expressed in M-HPL1 (Fig. 4a). We now need to examine whether PDL cells isolated from other MFS1 patients reveal a similar down-regulation of these genes.

Recently, attempts have been made to establish immortalized PDL cells by introducing *hTERT* (Berry et al. 2003; Kamata et al. 2004; Fujita et al. 2005; Saito et al. 2005; Fujii et al. 2006; Zhang et al. 2006). Cyclin-dependent kinase inhibitors $p16^{Ink4a}$ and $p21^{WAF1}$ induce premature senescence in human cells by telomere-independent mechanisms (Ramirez et al. 2001). As Bmi-1 can down-regulate the expression of $p16^{Ink4a}$ and $p14^{ARF}$ (Jacobs et al. 1999), it has been used to extend the life span of bovine and human cells (Dimri et al. 2002; Cudre-Mauroux et al. 2003; Itahana et al. 2003; Saito et al. 2005; Haga et al. 2007). Thus, in this study, we have immortalized human PDL cells with retrovirus-mediated transduction of both *hTERT* and *Bmi-1*. By using this method, both HPDL2 and M-HPL1 have been immortalized while maintaining their original gene expressions (Fig. 2c, Fig. 4a), as reported in cementoblast progenitor cells (Saito et al. 2005).

In MFS1, the activation of TGF-β signaling has been suggested as the pathogenesis for mitral valve prolapse and emphysema (Neptune et al. 2003; Ng et al. 2004). Mutations in *FBN1* alter or preclude matrix alteration of the latent complex of TGF-β, rendering TGF-β more accessible for activation (Neptune et al. 2003). In this study, activated TGF-β has been shown to be more abundant in M-HPL1 than in HPDL2 (Fig. 6e, f), suggesting that activated TGF-β signaling occurs in the PDL of our MFS1 patient.

N2144S in fibrillin-1 is predicted to alter one of the key calcium-binding residue ligands within the 32th cbEGF domain (Kettle et al. 1999; Yuan et al. 2002). This mutation is known to increase flexibility in the peptide backbone (Yuan et al. 2002). Attempts should be made to link this mutation and the disorganized cell alignment and microfibril assembly seen in this study.

OPN expression is lower in M-HPL1 than in HPDL2 (Fig. 4a). The exact reason for this difference is not known. However, TGF-β blockade has been reported significantly to enhance the BMP-2-induced upregulation of *OPN* expression, suggesting that TGF-β is a negative regulator on *OPN* expression (Shen et al. 2007). An examination is required of whether decreased expression of *OPN* (Fig. 4a) is mediated by the enhanced TGF-β activation in M-HPL1 (Fig. 6). Moreover, since no study has reported a relationship between fibrillin-1 and *OPN* expression, an investigation of *OPN* expression in M-HPL1 would be of interest after transfecting wild-type fibrillin-1 or during the culture of these cells on the fibrillin-1-coated dishes.

In summary, PDL cells have been isolated from an MFS1 patient with a heterozygous mutation in the 32th cbEGF domain (N2144S). These PDL cells have been immortalized by transducing human *mi-1* and *hTERT*. The present immortalized PDL cells show increased levels of activated TGF-β and should provide a powerful tool for the clarification of the biological roles of the elastic system fibers in PDLs and the pathogenesis of periodontitis in MFS1.

Acknowledgements The authors thank Dr. K. Ohyama (former Professor of Tokyo Medical and Dental University), Dr. S. Yamada (Osaka University), and Professor S. Murakami (Osaka University) for their valuable advice and discussion. The authors are also grateful to Professor T. Yoda (Saitama Medical University) and Dr. Y. Fukushima (Saitama Medical University) for organizing the tooth samples and providing the medical history of the patient. The authors also express their gratitude to Marfan Network Japan (MNJ) for their cooperation in the present research. Additional thanks are extended to Dr. T. Yokoi (Aichi Gakuin University), Dr. T. Tsubakimoto (Kanagawa Dental College), Dr. E. Nishida (Aichi Gakuin University), Dr. K. Kosaka (Kanagawa Dental College), and Dr. M. Aino (Aichi Gakuin University) for their technical assistance.

References

Bauss O, Sadat-Khonsari R, Fenske C, Engelke W, Schwestka-Polly R (2004) Temporomandibular joint dysfunction in Marfan syndrome. Oral Surg Oral Med Oral Pathol Oral Radiol Endod 97:592–598

Beertsen W, McCulloch CA, Sodek J (1997) The periodontal ligament: a unique, multifunctional connective tissue. Periodontol 2000:20–40

Berry JE, Zhao M, Jin Q, Foster BL, Viswanathan H, Somerman MJ (2003) Exploring the origins of cementoblasts and their trigger factors. Connect Tissue Res 44 (Suppl 1):97–102

Boileau C, Jondeau G, Babron MC, Coulon M, Alexandre JA, Sakai L, Melki J, Delorme G, Dubourg O, Bonaiti-Pellie C, Bourdarias JP, Junienet C (1993) Autosomal dominant Marfan-like connective-tissue disorder with aortic dilation and skeletal anomalies not linked to the fibrillin genes. Am J Hum Genet 53:46–54

Chien HH, Lin WL, Cho MI (1999) Interleukin-1beta-induced release of matrix proteins into culture media causes inhibition of mineralization of nodules formed by periodontal ligament cells in vitro. Calcif Tissue Int 64:402–413

Cho MI, Matsuda N, Lin WL, Moshier A, Ramakrishnan PR (1992) In vitro formation of mineralized nodules by periodontal ligament cells from the rat. Calcif Tissue Int 50:459–467

Cudre-Mauroux C, Occhiodoro T, Konig S, Salmon P, Bernheim L, Trono D (2003) Lentivector-mediated transfer of Bmi-1 and telomerase in muscle satellite cells yields a Duchenne myoblast cell line with long-term genotypic and phenotypic stability. Hum Gene Ther 14:1525–1533

Dietz HC, Cutting GR, Pyeritz RE, Maslen CL, Sakai LY, Corson GM, Puffenberger EG, Hamosh A, Nanthakumar EJ, Curristin SM, Stetten G, Meyers DA, Francomano CA (1991) Marfan syndrome caused by a recurrent de novo missense mutation in the fibrillin gene. Nature 352:337–339

Dimri GP, Martinez JL, Jacobs JJ, Keblusek P, Itahana K, Van Lohuizen M, Campisi J, Wazer DE, Band V (2002) The Bmi-1 oncogene induces telomerase activity and immortalizes human mammary epithelial cells. Cancer Res 62:4736–4745

Flanders KC, Thompson NL, Cissel DS, Van Obberghen-Schilling E, Baker CC, Kass ME, Ellingsworth LR, Roberts AB, Sporn MB (1989) Transforming growth factor-beta 1: histochemical local-

ization with antibodies to different epitopes. J Cell Biol 108: 653–660
Freeman E (1998) Periodontium. In: Ten Cate AR (ed) Oral histology: development, structure, and function, 5th edn. Mosby, St. Louis, pp 253–286
Fujii S, Maeda H, Wada N, Kano Y, Akamine A (2006) Establishing and characterizing human periodontal ligament fibroblasts immortalized by SV40T-antigen and hTERT gene transfer. Cell Tissue Res 324:117–125
Fujita T, Otsuka-Tanaka Y, Tahara H, Ide T, Abiko Y, Mega J (2005) Establishment of immortalized clonal cells derived from periodontal ligament cells by induction of the hTERT gene. J Oral Sci 47:177–184
Fullmer HM, Sheetz JH, Narkates AJ (1974) Oxytalan connective tissue fibers: a review. J Oral Pathol 3:291–316
Giannopoulou C, Cimasoni G (1996) Functional characteristics of gingival and periodontal ligament fibroblasts. J Dent Res 75: 895–902
Haga K, Ohno S, Yugawa T, Narisawa-Saito M, Fujita M, Sakamoto M, Galloway DA, Kiyono T (2007) Efficient immortalization of primary human cells by p16-specific short hairpin RNA or Bmi-1, combined with introduction of hTERT. Cancer Sci 98: 147–154
Handa K, Saito M, Yamauchi M, Kiyono T, Sato S, Teranaka T, Sampath Narayanan A (2002) Cementum matrix formation in vivo by cultured dental follicle cells. Bone 31:606–611
Hewett DR, Lynch JR, Smith R, Sykes BC (1993) A novel fibrillin mutation in the Marfan syndrome which could disrupt calcium binding of the epidermal growth factor-like module. Hum Mol Genet 2:475–477
Itahana K, Zou Y, Itahana Y, Martinez JL, Beausejour C, Jacobs JJ, Van Lohuizen M, Band V, Campisi J, Dimri GP (2003) Control of the replicative life span of human fibroblasts by p16 and the polycomb protein Bmi-1. Mol Cell Biol 23:389–401
Jacobs JJ, Kieboom K, Marino S, DePinho RA, Lohuizen M van (1999) The oncogene and Polycomb-group gene bmi-1 regulates cell proliferation and senescence through the ink4a locus. Nature 397:164–168
Kamata N, Fujimoto R, Tomonari M, Taki M, Nagayama M, Yasumoto S (2004) Immortalization of human dental papilla, dental pulp, periodontal ligament cells and gingival fibroblasts by telomerase reverse transcriptase. J Oral Pathol Med 33:417–423
Kapila YL, Kapila S, Johnson PW (1996) Fibronectin and fibronectin fragments modulate the expression of proteinases and proteinase inhibitors in human periodontal ligament cells. Matrix Biol 15:251–261
Kawamoto T, Shimizu M (2000) A method for preparing 2- to 50-micron-thick fresh-frozen sections of large samples and undecalcified hard tissues. Histochem Cell Biol 113:331–339
Kettle S, Yuan X, Grundy G, Knott V, Downing AK, Handford PA (1999) Defective calcium binding to fibrillin-1: consequence of an N2144S change for fibrillin-1 structure and function. J Mol Biol 285:1277–1287
Kielty CM, Sherratt MJ, Shuttleworth CA (2002) Elastic fibres. J Cell Sci 115:2817–2828
Kosaki K, Udaka T, Okuyama T (2005) DHPLC in clinical molecular diagnostic services. Mol Genet Metab 86:117–123
Kyo S, Nakamura M, Kiyono T, Maida Y, Kanaya T, Tanaka M, Yatabe N, Inoue M (2003) Successful immortalization of endometrial glandular cells with normal structural and functional characteristics. Am J Pathol 163:2259–2269
Maslen CL, Corson GM, Maddox BK, Glanville RW, Sakai LY (1991) Partial sequence of a candidate gene for the Marfan syndrome. Nature 352:334–337
Mecham RP (1991) Elastin synthesis and fiber assembly. Ann N Y Acad Sci 624:137–146
Miyazono K, Ichijo H, Heldin CH (1993) Transforming growth factor-beta: latent forms, binding proteins and receptors. Growth Factors 8:11–22
Mizuguchi T, Collod-Beroud G, Akiyama T, Abifadel M, Harada N, Morisaki T, Allard D, Varret M, Claustres M, Morisaki H, Ihara M, Kinoshita A, Yoshiura K, Junien C, Kajii T, Jondeau G, Ohta T, Kishino T, Furukawa Y, Nakamura Y, Niikawa N, Boileau C, Matsumoto N (2004) Heterozygous TGFBR2 mutations in Marfan syndrome. Nat Genet 36:855–860
Neptune ER, Frischmeyer PA, Arking DE, Myers L, Bunton TE, Gayraud B, Ramirez F, Sakai LY, Dietz HC (2003) Dysregulation of TGF-beta activation contributes to pathogenesis in Marfan syndrome. Nat Genet 33:407–411
Ng CM, Cheng A, Myers LA, Martinez-Murillo F, Jie C, Bedja D, Gabrielson KL, Hausladen JM, Mecham RP, Judge DP, Dietz HC (2004) TGF-beta-dependent pathogenesis of mitral valve prolapse in a mouse model of Marfan syndrome. J Clin Invest 114: 1586–1592
Nohutcu RM, McCauley LK, Koh AJ, Somerman MJ (1997) Expression of extracellular matrix proteins in human periodontal ligament cells during mineralization in vitro. J Periodontol 68:320–327
Nollen GJ, Mulder BJ (2004) What is new in the Marfan syndrome? Int J Cardiol 97 (Suppl 1):103–108
Pyeritz RE (2000) The Marfan syndrome. Annu Rev Med 51:481–510
Ramirez RD, Morales CP, Herbert BS, Rohde JM, Passons C, Shay JW, Wright WE (2001) Putative telomere-independent mechanisms of replicative aging reflect inadequate growth conditions. Genes Dev 15:398–403
Saito Y, Yoshizawa T, Takizawa F, Ikegame M, Ishibashi O, Okuda K, Hara K, Ishibashi K, Obinata M, Kawashima H (2002) A cell line with characteristics of the periodontal ligament fibroblasts is negatively regulated for mineralization and Runx2/Cbfa1/Osf2 activity, part of which can be overcome by bone morphogenetic protein-2. J Cell Sci 115:4191–4200
Saito M, Handa K, Kiyono T, Hattori S, Yokoi T, Tsubakimoto T, Harada H, Noguchi T, Toyoda M, Sato S, Teranaka T (2005) Immortalization of cementoblast progenitor cells with Bmi-1 and TERT. J Bone Miner Res 20:50–57
Sawada T, Sugawara Y, Asai T, Aida N, Yanagisawa T, Ohta K, Inoue S (2006) Immunohistochemical characterization of elastic system fibers in rat molar periodontal ligament. J Histochem Cytochem 54:1095–1103
Shen ZJ, Kim SK, Jun DY, Park W, Kim YH, Malter JS, Moon BJ (2007) Antisense targeting of TGF-beta1 augments BMP-induced upregulation of osteopontin, type I collagen and Cbfa1 in human Saos-2 cells. Exp Cell Res 313:1415–1425
Sherr CJ, DePinho RA (2000) Cellular senescence: mitotic clock or culture shock? Cell 102:407–410
Shiga M, Kapila YL, Zhang Q, Hayami T, Kapila S (2003) Ascorbic acid induces collagenase-1 in human periodontal ligament cells but not in MC3T3-E1 osteoblast-like cells: potential association between collagenase expression and changes in alkaline phosphatase phenotype. J Bone Miner Res 18:67–77
Staszyk C, Gasse H (2004) Oxytalan fibres in the periodontal ligament of equine molar cheek teeth. Anat Histol Embryol 33:17–22
Straub AM, Grahame R, Scully C, Tonetti MS (2002) Severe periodontitis in Marfan's syndrome: a case report. J Periodontol 73: 823–826
Ten Cate AR (1998) Hard tissue formation and destruction. In: Ten Cate AR (ed) Oral histology: development, structure, and function, 5th edn. Mosby, St. Louis, pp 69–77
Udaka T, Samejima H, Kosaki R, Kurosawa K, Okamoto N, Mizuno S, Makita Y, Numabe H, Toral JF, Takahashi T, Kosaki K (2005) Comprehensive screening of CREB-binding protein gene mutations among patients with Rubinstein-Taybi syndrome using

denaturing high-performance liquid chromatography. Congenit Anom 45:125–131

Westling L, Mohlin B, Bresin A (1998) Craniofacial manifestations in the Marfan syndrome: palatal dimensions and a comparative cephalometric analysis. J Craniofac Genet Dev Biol 18:211–218

Yamada S, Murakami S, Matoba R, Ozawa Y, Yokokoji T, Nakahira Y, Ikezawa K, Takayama S, Matsubara K, Okada H (2001) Expression profile of active genes in human periodontal ligament and isolation of PLAP-1, a novel SLRP family gene. Gene 275:279–286

Yokoi T, Saito M, Kiyono T, Iseki S, Kosaka K, Nishida E, Tsubakimoto T, Harada H, Eto K, Noguchi T, Teranaka T (2007) Establishment of immortalized dental follicle cells for generating periodontal ligament in vivo. Cell Tissue Res 327:301–311

Yuan X, Werner JM, Lack J, Knott V, Handford PA, Campbell ID, Downing AK (2002) Effects of the N2144S mutation on backbone dynamics of a TB-cbEGF domain pair from human fibrillin-1. J Mol Biol 316:113–125

Zhang X, Soda Y, Takahashi K, Bai Y, Mitsuru A, Igura K, Satoh H, Yamaguchi S, Tani K, Tojo A, Takahashi TA (2006) Successful immortalization of mesenchymal progenitor cells derived from human placenta and the differentiation abilities of immortalized cells. Biochem Biophys Res Commun 351:853–859

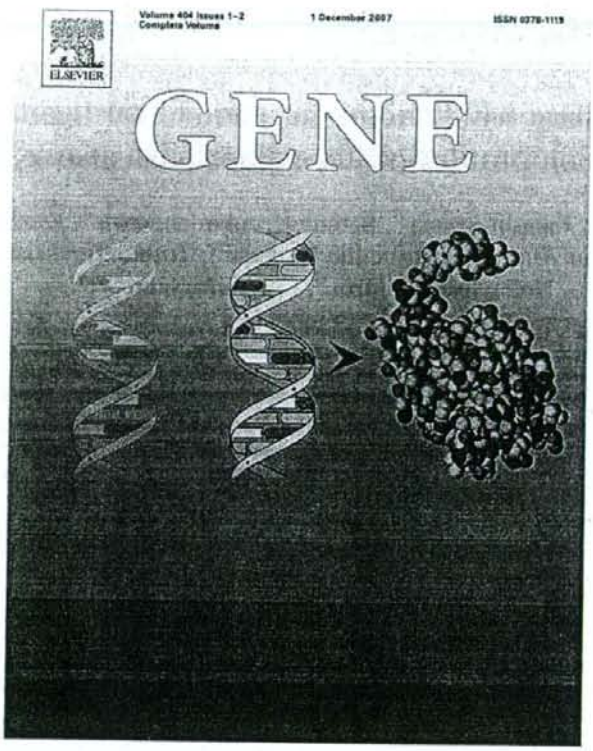

Available online at www.sciencedirect.com
ScienceDirect
Gene 404 (2007) 70–79
GENE
www.elsevier.com/locate/gene

Transcriptome database KK-Periome for periodontal ligament development: Expression profiles of the extracellular matrix genes

Eisaku Nishida [a,b,c], Takashi Sasaki [d], Sabine Kazuko Ishikawa [d], Kazutaka Kosaka [a,b], Makoto Aino [a,b,c], Toshihide Noguchi [c], Toshio Teranaka [a], Nobuyoshi Shimizu [d], Masahiro Saito [a,b,*]

[a] Department of Operative Dentistry and Endodontics, Kanagawa Dental College, Kanagawa, Japan
[b] Oral Health Science Research Center, Kanagawa Dental College, Yokosuka, Kanagawa, Japan
[c] Department of Periodontology, School of Dentistry, Aichi-Gakuin University, Aichi, Japan
[d] Department of Molecular Biology, Keio University School of Medicine, Tokyo, Japan

Received 18 June 2007; received in revised form 3 September 2007; accepted 4 September 2007
Available online 19 September 2007
Received by Takashi Gojobori

Abstract

Specialized connective tissues such as tendon/ligament develop through a series of events that require temporal and spatial expression of numerous genes in mesenchymal progenitors. However, the genes required for tendon/ligament development have not been identified yet. To solve this problem, we made a cDNA library from periodontal ligament and sequenced 11,520 cDNA clones, as a model for investigating tendon/ligament development. The resulting sequence data was assembled to 617 expressed sequence tag (EST) clusters, and an EST database for human periodontal ligament (PDL) was constructed (designated as the KK-Periome database). In the KK-Periome database, the top 13 EST clusters were related to extracellular matrix (ECM) genes. The temporal and spatial expression patterns of these genes during mouse PDL development were examined by *in situ* hybridization. Among these genes, *F-spondin* was expressed specifically in dental follicle (DF) cells during tooth germ development, whereas *tenascin-N* was strongly expressed in the terminally differentiated PDL. This characteristic expression profile was confirmed by *in vivo* differentiation assay of human PDL (hPDL) cells in the mouse transplant. Thus, the KK-Periome database was proven to be a useful resource for PDL-derived ESTs (transcriptome), and in fact, initial evidence indicated that *F-spondin* and *tenascin-N* might serve as markers for DF and PDL, respectively.

Keywords: EST library; Database; Expression patterning; Connective tissue; Extracellular matrix; Periodontal ligament

1. Introduction

Periodontium is a tooth supporting tissue composed of periodontal ligament (PDL), cementum and alveolar bone. More specifically, the PDL is composed of densely packed collagen-rich connective tissue capable of withstanding occlusal force. Collagen type I is predominant, but collagen types III, IV, V, VI and XII and proteoglycans are also deposited into the PDL extracellular matrix (Huang et al., 1991; Karimbux et al., 1992; Lukinmaa et al., 1992; Ten Cate, 1994; Matheson et al., 2005; McCulloch, 2006). In periodontitis, a chronic inflammatory disease that affects the periodontium, the PDL is irreversibly damaged. Despite a number of novel approaches, it has not yet been possible to reliably regenerate the PDL (D'Errico et al., 1999). Hence, there is considerable interest in the developmental mechanisms of PDL.

PDL originates from dental follicle (DF) cells that form on the embryonic day 14 (E14) of tooth germ development. During tooth germ development, DF cells differentiate into progenitors of

Abbreviations: DF, Dental follicle; ECM, Extracellular Matrix; EST, Expressed Sequence Tag; PDL, Periodontal Ligament.

* Corresponding author. Department of Molecular and Cellular Biochemistry, Osaka University Graduate School of Dentistry, 1-8 Yamadaoka, Suita, Osaka 565-0871, Japan. Tel.: +81 6 6879 2888; fax: +81 6 6879 2890.
E-mail address: mssaito@dent.osaka-u.ac.jp (M. Saito).

0378-1119/$ - see front matter © 2007 Elsevier B.V. All rights reserved.
doi:10.1016/j.gene.2007.09.009

Table 1
List of primers used in preparation of probe for *in situ* hybridization

Gene symbol	Gene product	Primer	
Col11a1	Collagen, type XI, alpha 1	Sense	5′-TTT CCC AAA CTT GCA CAT GA-3′
		Antisense	5′-CAC GCT GAG GAC AAT GAA GA-3′
Sparcl1	SPARC-like 1	Sense	5′-AAT GAA CTG GAC CAG CAT CC-3′
		Antisense	5′-AAA CGC AGA TGC ACA GAG TG-3′
Tnn	Tenascin-N	Sense	5′-CAA GAC CTG GAA CAG GGT GT-3′
		Antisense	5′-TGC CTC TGT ATT TCC CAA CC-3′
Col15a1	Collagen, type XV, alpha 1	Sense	5′-AAT CCG TAT CAG CCA CAA CC-3′
		Antisense	5′-TCC AGA ATC TTC CCT GTG CT-3′
Hapln1	Hyaluronan and proteoglycan link protein 1	Sense	5′-CAA GCA GAG AAG AGT CTG AG-3′
		Antisense	5′-GTT CTG CTT CCA CAA GTA GAC-3′
Vit	Vitrin	Sense	5′-CGA ATT TGG GTT CGA CAA GT-3′
		Antisense	5′-GAG CTC CTA GCC AGC CTT TT-3′
Col16a1	Collagen, type XVI, alpha 1	Sense	5′-TAC CTC CAG GAT GCA GTT CC-3′
		Antisense	5′-TCC TGT AAG CTT TGG CCA TT-3′
Smoc2	SPARC related modular calcium binding 2	Sense	5′-ATC CAA GCC CAA AAA GTG TG-3′
		Antisense	5′-AGG GCA AGG GAA TAA ACC AG-3′
Grn	Granulin	Sense	5′-ATG CTG TGT GCT GTG AGG AC-3′
		Antisense	5′-GTC CAC AGA AAC CGG AAG AA-3′
Fbln5	Fibulin 5	Sense	5′-AGG GGC GAC TAC CAT TTC TT-3′
		Antisense	5′-TGC GGC TAC CAC ACT AAT GA-3′
Spon1	Spondin 1	Sense	5′-AGA CGG TCT ACT GGG CAC TG-3′
		Antisense	5′-TGC AAA AGG ATG TGG TGG TA-3′
Nid1	Nidogen 1	Sense	5′-ACG TCA TGG GAA TCT TCA GC-3′
		Antisense	5′-TGC AAA CCG AAC TTC TGA TG-3′
Lepre1	Leprecan 1	Sense	5′-GTC ACA GGC TGA GAG GAA GG-3′
		Antisense	5′-GCC CAG AGA AGA GTG TGT CC-3′
TNN	Human tenascin-N	Sense	5′-AAG ACC AGA GGT TTG CGT TG-3′
		Antisense	5′-GCT TAT ACC GCT CCT TGC TG-3′

periodontium lineage including PDL-progenitors. Differentiation of PDL-progenitors is initiated in the tooth root-forming stage of the tooth germ, and PDL formation is completed when the tooth erupts. Thus, DF provides a useful experimental model to investigate the differentiation mechanisms of PDL (Yokoi et al., 2007). However, the precise differentiation mechanism of DF remains to be determined as the specific marker that distinguishes DF and PDL is not available. Therefore, it is important to identify the PDL cell lineage-specific markers to clarify the mechanism of DF cell differentiation.

The phenotypic property of a cell is determined by the unique combination of the expressed gene products. Therefore, the gene expression profile provides an informative modality to define the cellular marker of each tissue. The recent availability of genomic sequence information and high-throughput advances allow transcriptional analysis of highly specified organs such as PDL. Expressed sequence tags (ESTs) are short single-pass sequence reads of randomly selected clones from cDNA library, and they are invaluable for identification of genes and gene expression pattern in a particular type of tissue (Venter et al., 2003). Thus, an EST database could provide a platform for identification of PDL-specific markers. Here, we established the EST database for human PDL and examined the spatial and temporal expression patterns of 13 representative ESTs during PDL development.

2. Methods

2.1. Construction of human PDL cDNA library

The human PDL cDNA library was constructed using Plasmid System with Gateway Technology for Complementary DNA (cDNA) Synthesis and Cloning, as described in the manufacturer's protocols. After obtaining informed consent and approval (approval number 18) of the Ethics Committee of Kanagawa Dental College, PDL from extracted third molars were harvested. Total RNA was extracted using ISOGEN (Nippon Gene Co., Ltd, Tokyo, Japan) from PDL tissue and poly(A)+ mRNA was obtained with μMACS mRNA Isolation Kit (Miltenyi Biotec Inc. Auburn, CA, USA), by following the manufacturer's protocols. cDNA was synthesized from poly(A)+ RNA with oligo dT primer using SuperScript Choice System (Invitrogen Corporation, Carlsbad, CA, USA), according to the manufacturer's instructions. The synthesized cDNA was separated based on size, and fractions > 1 kbp were inserted into the *SalI*/*NotI* restriction site of pBluescriptSK(−) plasmid (Stratagene, La Jolla, CA, USA). The ligated DNA was electroporated into competent *E. coli* cells (DH10B) by using E-coli Pulser (Bio-Rad Hercules, CA, USA).

2.2. DNA Sequencing and sequence data analysis

The plasmid DNA in transformed *E. coli* was amplified directly using TempliPhi DNA amplification kit (GE Healthcare, Piscataway, NJ, USA), and then cycle sequencing reactions were performed using M13 primer and Big Dye (v3.1). These were subjected to a 3730 DNA analyzer (Applied Biosystems, Foster City, CA, USA). A total of 11,520 clones from human PDL library were sequenced to obtain 5′EST. After trimming the vector sequence using the cross-match software, clustering of ESTs within a library was assembled by CAP3 sequence assembly program (Huang and Madan, 1999). To identify the gene

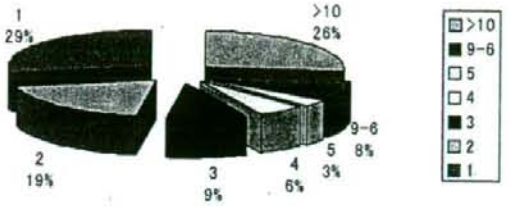

Fig. 1. Classification of ESTs according to their expression frequency. ESTs obtained by the sequencing analysis of human PDL cDNA library were classified according to their expression frequency (The number of same EST clones range from 1 to >10).

corresponding to each EST cluster, non-redundant clusters were analyzed against RefSeq data by BLAST (www.ncbi.nlm.nih.gov/BLAST). For the functional classification of each EST cluster, we used data of the gene ontology from Genecards (http://www.genecards.org/index.shtml), Ensembl (http://www.ensembl.org), and Genebank (http://www.ncbi.nlm.nih.gov).

2.3. Probes for in situ hybridization

The mouse homologues of the candidate EST clusters were searched from homologene (http://www.ncbi.nlm.nih.gov/entrez/query.fcgi?db=homologene). Specific primer for amplification of mouse cDNA is listed in Table 1. After amplification of cDNA by RT-PCR, the PCR product was subsequently cloned into pCR4 TOPO vector (Invitrogen Corporation, Carlsbad, CA, USA). The plasmid DNAs were linearized by *Not* I (antisense) or *Spe* I (sense) for *in situ* hybridization. The probe for periostin was used for control, as described previously (Yokoi et al., 2007).

2.4. In situ hybridization

To generate antisense and sense transcripts, digoxygenin-labeled riboprobes were prepared using T7 or T3 RNA polymerase, as described elsewhere (Wilkinson, 1995). Heads of C57BL mice at embryonic (E) 13 days, E15, E17 and postnatal (P) 1 day were immediately frozen after embedding in OCT compound (Sakura Fine Technical Co., Ltd., Tokyo, Japan) and 10-μm sagittal sections were made. Mandibles of 35-day postnatal mice were fixed in 4% paraformaldehyde at 4 °C overnight, decalcified with Morse's solution (Shibata et al., 2000) for 24 h, then embedded in OCT compound, and 10-μm sagittal sections were made. *In situ* hybridization was carried out on these sections, as previously described with slight modification (Iseki et al., 1997). Polyvinyl alcohol was used as buffer during color reaction. Serial sections were made and *in situ* hybridization analysis was carried out 3 times per probe and stage.

Table 2
Functional categorization of EST clusters in the KK-Periome database

1. Known function clusters	481 (78%)
(1) Ribosomal proteins	19 (3%)
(2) Initiation/elongation factors	9 (1%)
(3) Cell cycle	18 (3%)
(4) Energy production	45 (7%)
(5) Extracellular matrix proteins	39 (6%)
(6) Plasma membrane proteins	44 (7%)
(7) Signaling molecules	12 (2%)
(8) Proteinase	12 (2%)
(9) Intracellular signaling	96 (15%)
(10) Transcriptional factors	40 (6%)
(11) Cytoskeleton-related proteins	25 (4%)
(12) Other functions	122 (20%)
2. Unknown function clusters	101 (16%)
3. Unknown transcript clusters	35 (6%)
Total clusters	617 (100%)

After redundancy analysis, the clusters that showed an expression frequency of more than three times were collected and perform functional annotation. Parameters of functional categorization and proportion are shown.

2.5. In vivo differentiation assay

Human PDL cells (hPDL), a kind gift from Dr. T. Kawase (Approval number 8 from the Ethics Committee of Kanagawa Dental College), were cultured in α-minimum essential medium (α-MEM; Sigma, St. Louis, MO, USA) containing 10% fetal bovine serum (FBS; BioWhittaker, Maryland, USA), 50 μg/ml of ascorbic acid, 100 units/ml of streptomycin and penicillin, in a humidified atmosphere of 5% CO_2 at 37 °C (Handa et al., 2002). Implantation of hPDL into SCID mice was carried out as described previously (Handa et al., 2002). Briefly, cells were inoculated subcutaneously into 5-week-old male CB-17 scid/scid (SCID) mice (Nihon Crea, Tokyo, Japan) after incubating 1.5×10^6 cells in a mixture of 40 mg of hydroxyapatite powder (Osferion; Olympus, Tokyo, Japan) and fibrin clot (mixture of mouse fibrinogen and thrombin: both from Sigma). Transplantation analysis was carried out 3 times, and 3 transplants were prepared per group. The mice were sacrificed after 4 weeks, and subjected to histochemical analysis with immunohistochemical staining or *in situ* hybridization as described below.

2.6. Histochemical analysis

The transplants were fixed in 4% paraformaldehyde for 1 day, decalcified with 12.5% EDTA containing 2.5% paraformaldehyde for 3 days and then embedded in OCT compound to produce frozen sections. Subsequently, 100 serial sections of 10-μm thickness were made per implant, and analyzed histochemically. Expression of mRNA for *tenascin-N* was examined by *in situ* hybridization as described above. In immunohistochemical analysis, to avoid nonspecific staining of mouse monoclonal antibodies, sections were blocked using the M.O.M kit (Vector Laboratories, Burlingame, CA, USA). The sections were incubated with anti-vimentin monoclonal antibody (V9; Dako, Carpinteria, CA, USA) for 1 h. Dilutions were made with PBS containing 2 mg/ml bovine serum albumin. The sections were incubated with nonimmune mouse IgG, which served as a control. After washing, fluorescence was observed by fluorescence microscopy (Axio Imager; Carl Zeiss, Jena, Germany).

2.7. RNA preparation and real time PCR analysis

Total RNA was isolated from cells using ISOGEN (Nippon Gene Co., Ltd.), as described previously (Handa et al., 2002).

Table 3
List of extracellular matrix ESTs expressed in the KK-Periome database

Frequency	Refseq ID	Gene symbol	Gene product	Reference
274	NM_000089	COL1A2	Collagen, type I, alpha 2	Lukinmaa et al. (1992)
156	NM_003118	SPARC	Secreted protein, acidic, cysteine-rich	Takano-Yamamoto et al.'(1994)
133	NM_000090	COL3A1	Collagen, type III, alpha 1	Tsubota et al. (2002)
81	NM_006475	POSTN	Periostin	Kruzynska-Frejtag et al. (2004)
65	NM_002345	LUM	Lumican	Hall et al. (1997)
62	NM_000088	COL1A1	Collagen, type I, alpha 1	Lukinmaa et al. (1992)
57	NM_000582	SPP1	Osteopontin	D'Errico et al. (1997)
43	NM_133506	DCN	Decorin	Matsuura et al. (2001)
24	NM_212482	FN1	Fibronectin	Hou et al. (1999)
21	NM_017680	ASPN	Asporin	Yamada et al. (2001)
19	NM_080645	COL12A1	Collagen, type XII, alpha 1	MacNeil, et al. (1998)
17	NM_000393	COL5A2	Collagen, type V, alpha 2	Lukinmaa and Waltimo (1992)
16	NM_014208	DSPP	Dentin sialophosphoprotein	D'Errico et al. (1997)
15	NM_057167	COL6A3	Collagen, type VI, alpha 3	Sloan et al. (1993)
*11	NM_080630	COL11A1	Collagen, type XI, alpha 1	
10	NM_004385	CSPG2	Versican	Shibata et al. (2002)
9	NM_002160	TNC	Tenascin C	Sahlberg et al. (2001)
8	NM_004967	IBSP	Bone sialoprotein	D'Errico et al. (1997)
8	NM_001711	BGN	Biglycan	Matsuura et al. (2001)
*6	NM_004684	SPARCL1	SPARC-like 1	
6	NM_000138	FBN1	Fibrillin 1	Sawada et al. (2006)
6	NM_005014	OMD	Osteomodulin	Petersson et al. (2003)
*6	NM_022093	TNN	Tenascin-N	
*5	NM_001855	COL15A1	Collagen, type XV, alpha 1	
*4	NM_001884	HAPLN1	Hyaluronan and proteoglycan link protein 1	
4	NM_004407	DMP1	Dentin matrix acidic phosphoprotein	Worapamorn et al. (2000)
*4	NM_053276	VIT	Vitrin	
4	NM_002290	LAMA4	Laminin, alpha 4	Salmivirta et al. (1997)
4	NM_006485	FBLN1	Fibulin 1	Sawada et al. (2006)
*4	NM_001856	COL16A1	Collagen, type XVI, alpha 1	
*3	NM_022138	SMOC2	SPARC related modular calcium binding 2	
*3	NM_002087	GRN	Granulin	
*3	NM_006329	FBLN5	Fibulin 5	
*3	NM_006108	SPON1	Spondin 1	
*3	NM_002508	NID1	Nidogen 1	
*3	NM_022356	LEPRE1	Leprecan 1	
3	NM_001849	COL6A2	Collagen, type VI, alpha 2	Sloan et al. (1993)
3	NM_000093	COL5A1	Collagen, type V, alpha 1	Lukinmaa and Waltimo (1992)

ESTs which are classified as an extracellular matrix, are listed according to frequency level.
Numbers given show the relative expression level of the ESTs. Asterisks show the gene clusters that have not been analyzed expression in the PDL.

cDNAs were synthesized from 1 μg of total RNA in a 20 μl reaction containing 10× reaction buffer, 1 mM dNTP mixture, 1 U/μl RNase inhibitor, 0.25 U/μl reverse transcriptase (M-MLV reverse transcriptase, (Invitrogen) and 0.125 μM random 9-mers (Takara, Tokyo, Japan). Normalization was performed using house keeping gene, glyceraldehyde-3-phosphate dehydrogenase (*GAPDH*) expression as an endogenous control in the same reaction as the gene of interest. The primers for real time PCR were designed with Primer 3 soft ware (http://frodo.wi.mit.edu/cgi-bin/primer3/primer3_www.cgi) based on the target gene. The details are; type XII collagen alpha1; sense 5′-GGA GAC AGA GGC TTC ACT GG -3′, antisense 5′-TCC TTT CAA CCC AGA TGG AC-3′, periostin; sense 5′-GAT GGA GTG CCT GTG GAA AT-3′, antisense 5′-TGG TGA CCT TGG TGA CCT CT-3′ antisense 5′-CCA AAG TTC CCA AGC TGA AC-3′, F-spondin; sense 5′-ACT CCA CAT GGA GAG GCA AC -3′, antisense 5′-AAG AGA TGG GCA AAC AAT GG-3′; tenascin-N; sense 5′-GCT CAG ATC CAC GGC TAC AT-3′, antisense 5′-GAC CAC CCT TAA AGG CAA CA-3′ and glyceraldehyde-3-phosphate dehydrogenase (*GAPDH*): sense 5′ -GTC AGT GGT GGA CCT GAC CT-3′, antisense 5′-TCG CTG TTG AAG TCA GAG GA-3′. For real time PCR, the reaction was performed with *Power* SYBR® Green PCR Master Mix (Applied Biosystems), and products were analyzed with AB 7300 Real-Time PCR System (Applied Biosystems).

3. Results

3.1. Sequence analysis of ESTs from human PDL cDNA library

In order to analyze the expression profile in human PDL cDNA library, a total of 11,520 cDNA clones were randomly selected, and sequenced from the 5′ ends. A total of 11,520 clones were sequenced from 5′ends, and 9600 high quality sequences were processed for further analysis. Redundancy analysis resulted in 4384 independent EST clusters. Expression frequency of each EST ranged from one to ten times or as high as 274 times (Fig. 1 and Table 3). We considered 617 EST

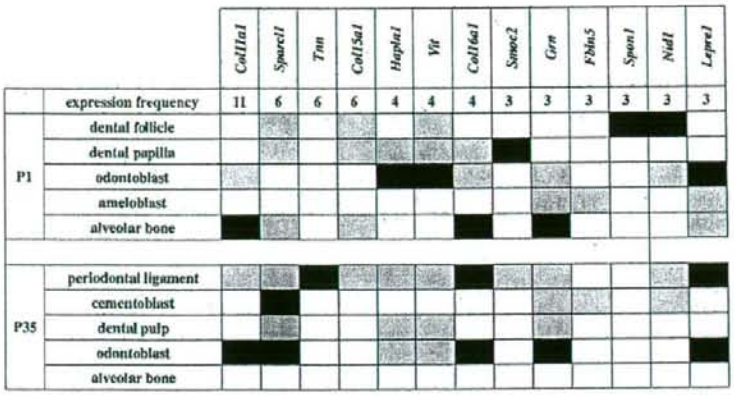

Fig. 2. *In situ* hybridization and expression frequency of 13 different ECMs in the developing tooth germ (P1) or adult periodontium (P35). *In situ* hybridization analysis of 13 ECM clusters in tooth germ at postnatal 1 day (P1) or adult periodontium (P35) are shown. ECM clusters are listed according to the expression frequency, type of cells in P1-tooth germ or P35-periodontium. Note that *F-spondin* (Spn1) is intensely expressed in the dental follicle cells. In contrast, *tenascin-N* (Tnn) is strongly expressed in the periodontal ligament. Black: strongly positive expression; Gray: weakly positive expression; White: No expression.

clusters with an expression frequency of more than 3 times as highly expressed genes in the PDL (Table 3).

3.2. Establishment of KK-Periome database

These 617 EST clusters were classified into 12 categories according to their ontology function (Table 2) (Yamada et al., 2001). Redundancy analysis identified 481 ESTs (78%) as known clusters, 101 ESTs (16%) as unknown function clusters and 35 ESTs (6%) as unknown transcript clusters, perhaps intra- and inter-genic transcripts. The largest category included secreting molecules such as ECMs, plasma membrane, proteases and protease inhibitors and signaling molecules (Table 2). The next abundant ESTs included genes involved in cellular signaling (such as ras homolog gene family member A, sorting nexin 17, and insulin-like growth factor binding protein 4), energy production (such as carboxypeptidase E, GNAS complex locus, ATP synthase H+ transporting, and mitochondrial F1 complex) and transcription factors (such as those similar to H3 histone family 3B, Y box binding protein 1, and HMT1 hnRNP methyltransferase-like 3).

3.3. Expression pattern of 13 extracellular matrix genes

We focused on ESTs for ECM in the KK-Periome database. As shown in Table 3, the top 10 transcripts were type I collagen alpha 2 (*COL1A2*), SPARC/osteonectin, collagen type III (*COL3A1*), periostin (*POSTN*), lumican (*LUM*), type I collagen alpha 2 chain (*COLIA1*), osteopontin (*SPP1*), decorin (*DCN*), fibronectin (*FN1*), and PLAP-1/Asporin (*ASPN*). These are major ECM components in PDL. The rest of ESTs include cementoblast/osteoblast markers such as bone sialoprotein (*IBSP*), osteomodulin (*OMD*) and dentin matrix acidic phosphoprotein 1 (*DMP1*) (D'Errico et al., 1997). To identify genes related to PDL formation, we screened the EST clusters, which are highly expressed during PDL development. For this purpose, the EST clusters which have been reported in PDL were selected by PubMed search and 13 EST clusters were obtained as candidates including collagen type XI alpha 1 (*COL11A1*), SPARC-like 1 (*SPARCL1*), tenascin-N (*TNN*), collagen type XV alpha 1 (*COL15A1*), hyaluronan and proteoglycan link protein 1 (*HAPLN1*), vitrin (*VIT*), type XVI collagen alpha 1 (*COL16A1*), SPARC related modular calcium binding 2 (*SMOC2*), granulin (*GRN*), fibulin 5 (*FBLN5*), F-spondin (*SPON1*), nidogen 1 (*NID1*) and leprecan 1 (*LERPE1*).

The mouse ortholog of human candidate genes was selected, and subjected to *in situ* hybridization analysis to examine whether they were expressed in P1-DF or in P35-PDL. The results of the analysis were classified according to expression frequency, postnatal stage and type of cells in P1-tooth germ or P35-periodontium (Fig. 2). F-spondin was expressed specifically in P1-DF, and no expression was found in other cell types in the P1-tooth germ, suggesting that it could serve as a proper marker. Nidogen 1 was also intensely expressed in DF as well as odontoblasts. The remaining candidate genes showed weak or no expression in DF, while they were expressed in other cells of the tooth germ. In P35-PDL, the expression patterns of candidate genes were significantly different from those of P1-DF. Expression of F-spondin and nidogen 1 was markedly decreased in P35-PDL, whereas expression of tenascin-N, type VI collagen alpha 1, and leprecan was strikingly up-regulated. Among the up-regulated genes, tenascin-N was highly restricted to P35-PDL, indicating that it could serve as a marker for PDL.

3.4. Expression pattern of F-spondin and tenascin-N

To determine whether F-spondin and tenascin-N are involved in the formation of PDL, we examined the expression pattern of these genes during PDL development. F-spondin was initially expressed in E15-DF cells surrounding dental epithelium (Fig. 3Ab) and became progressively evident in the E17 and P1 DF cells (Fig. 3A, c and d). However, expression of F-spondin was significantly down-regulated in P7-DF cells, and no expression was detected in P35-PDL (Fig. 3B, a and b). In contrast, expression of tenascin-N

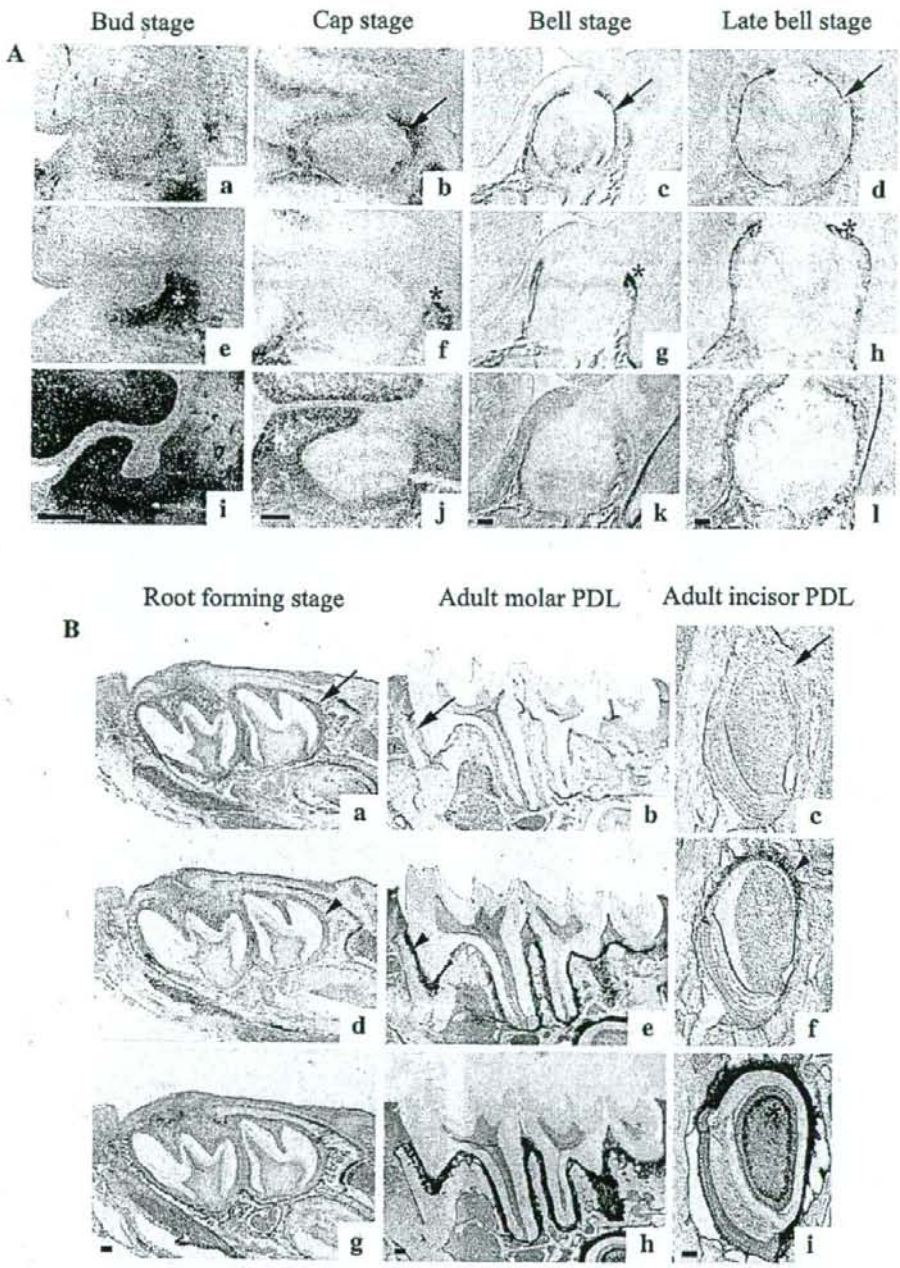

Fig. 3. Expression patterns of F-spondin and tenascin-N during early tooth germ development or tooth root formation. (A) During tooth germ development: F-spondin is initially expressed at the cap stage of DF in the tooth germ (b: arrow), and became intensely expressed in the bell stage and late stage of the DF (c and d: arrows). In contrast, expression of tenascin-N is not detected in the DF (e–h). However, tenascin-N expression is observed in dental mesenchymal cells at E13-bud stage (e: asterisk), and is also expressed in periosteum. E15-cap stage to P1-late bell stage (f–h: asterisks). Expression of periostin can been seen in dental mesenchyme in E13 tooth germ (i), and in DF during tooth germ development (j–l). bar: 100 μm. (B) During tooth root formation: F-spondin is weakly expressed in root-forming stage of DF at P7 (a: arrow) and is not expressed in P35-adult molar PDL (b: arrow) as well as in adult incisor lingual side (c: arrow). Tenascin-N is not expressed in P7-root-forming stage of DF (d), however the expression was intensely up-regulated in P35-adult molar PDL (e: arrowhead). Specific expression of tenascin-N is also observed in adult incisor lingual side (f, arrowhead) although no expression is found in the labial side (f). Expression of periostin was observed in DF (g) and P35-adult molar PDL (h), but it is also detected in the preodontoblast layer (i: asterisk). bar: 100 μm.

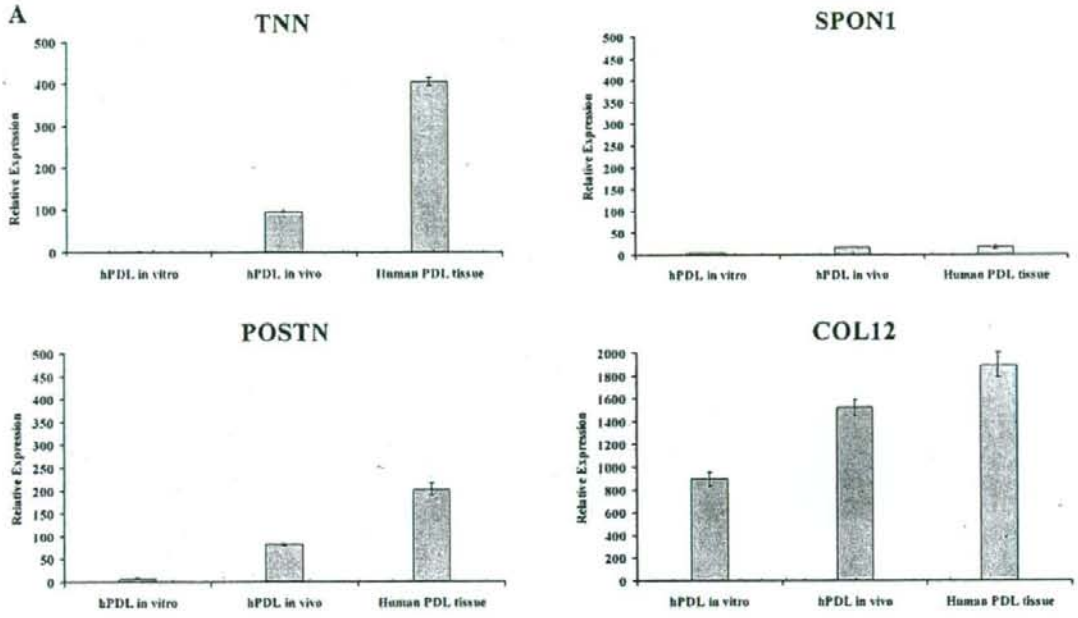

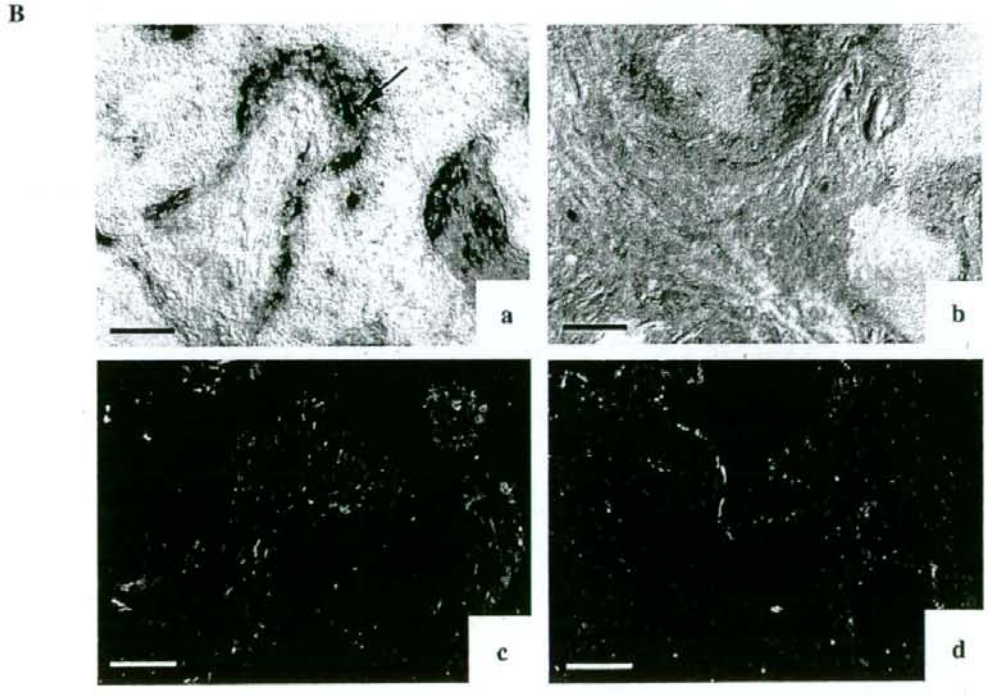

could not be detected in the DF cells at E15, E17, P1and P7-DF of the developing tooth germ, (Fig. 3A, e–h, and Bd), but it was intensely up-regulated in the P35-PDL region where PDL cells enter terminal differentiation (Fig. 3Be). Mouse incisor showed asymmetrical distribution of PDL on the lingual side while no formation was found on the labial side. In the mouse incisor at P35, significant expression of tenascin-N was detected on the lingual side (Fig. 3Bf, arrowhead), whereas no expression was observed on the labial side (Fig. 3Bf). In contrast to tenascin-N, expression of F-spondin could not be detected in this region (Fig. 3Bc). In the control experiment, intense expression of periostin was observed in E13 dental mesenchyme and surrounding tissue (Fig. 3Ai). Consequently, periostin was expressed in DF at E15, E17 and P1-tooth germ (Fig. 3A, j–l). During tooth root-forming stage, periostin was expressed in DF, and strongly expressed in P35-PDL (Fig. 3B, g and h). However, strong expression was also detected in the preodontoblast layer of adult incisor (Fig. 3Bi).

3.5. In vivo differentiation of hPDL cells

Previous work has demonstrated that differentiation of cultured hPDL cells is induced upon implantation of these PDL cells into immunodeficient mice (Handa et al., 2002; Seo et al., 2004). We examined the expression of F-spondin and tenascin-N in cultured hPDL cells by real time PCR analysis to determine whether these genes are involved in differentiation of hPDL cells. Tenascin-N expression was not detected in cultured hPDL, but it was significantly induced in cells of the hPDL transplant 4 weeks after implantation (Fig. 4A). Contrary to tenascin-N, the expression of F-spondin in the cultured hPDL cells did not significantly differ from that in the hPDL transplant (Fig. 4A). In the control experiment, periostin expression slightly increased in the hPDL transplant (Fig. 4A). We also examined the mRNA expression level of type XII collagen as a control for PDL differentiation (Karimbux et al., 1992). Intense expression of type XII collagen was detected in cultured hPDL cells and it increased in the hPDL transplant (Fig. 4A). Expression patterns of these genes in the hPDL transplant were similar to that in human PDL tissue, indicating that hPDL cell differentiation was induced upon implantation into mouse (Fig. 4A). No expression of human tenascin-N, F-spondin, periostin and type XII collagen was detected in the transplants without human cells (data not shown). Expression of tenascin-N in the cells of the hPDL transplant was confirmed by *in situ* hybridization analysis. Results showed that significant tenascin-N expression was induced in the cells of the hPDL transplant (Fig. 4Ba). In addition, cells of the hPDL transplant were positive for antibody against human specific vimentin (Fig. 4Bc). In the control site without implantation of hPDL cells, no positive signals were detected for tenascin-N and vimentin (Fig. 4B, b and d).

4. Discussion

4.1. Establishment of KK-Periome database and classification of ECM genes

Previous research has provided information on the expression of ECM genes during PDL formation (Karimbux et al., 1992; Takano-Yamamoto et al., 1994; Kruzynska-Frejtag et al., 2004). However, we still have limited knowledge regarding the transcriptional control of PDL development. Knowing the complexity of the process of PDL development, establishment of a gene expression profile database was considered useful, to identify the genes that play critical roles in the cascades of PDL development. Hence, we established the KK-Periome database that represents a collection of transcripts that are highly expressed in the human PDL. In the database, we found that unique ECM components such as F-spondin and tenascin-N are expressed at specific stages of DF and PDL during development. F-spondin was expressed in the early stage of DF, whereas tenascin-N expression was strongly induced upon PDL differentiation, suggesting that these genes/proteins represent markers for DF and PDL, respectively. Thus, the KK-Periome database has a potential to provide useful transcriptome information for investigating gene expression during PDL formation.

It was previously reported that PDL possessed a stem cell population that can differentiate into PDL, osteoblast and adipocyte (Seo et al., 2004). We also reported that a progenitor that can form PDL tissue was present in DF and PDL (Saito et al., 2005; Handa et al., 2002). From these findings, we hypothesized that both differentiated PDL-specific and immature PDL such as DF-specific markers could be identified from the KK-Periome database. To identify these markers, EST clusters in the KK-Periome database were analyzed by three different parameters such as expression frequency, functional classification and expression pattern: (1) EST clusters with expression frequency of more than three times were selected for inclusion in the KK-Periome database. (2) Since ECM is involved in tissue specificity, a list of ECM clusters was analyzed to determine whether the KK-Periome database reflects PDL phenotype. (3) Candidate genes that may play critical roles in the process of PDL development were selected

Fig. 4. Expression of F-spondin and tenascin-N in human periodontal ligament (hPDL) cells *in vitro* and *in vivo*. (A) Real time PCR analysis for tenascin-N (TNN),F-spondin (SPON), periostin (POSTN) and type XII collagen (COL12) and GAPDH *in vitro* and *in vivo*. Total RNA was isolated from hPDL cells (hPDL *in vitro*), hPDL cells of the transplant (hPDL *in vivo*) and human PDL tissue and subjected to real time PCR analysis. Level of TNN, SPON, POSTN and COL12A1 mRNA expression level were normalized against GAPDH level. Level of GAPDH mRNA expression was set at 100, and relative expression level was shown. Expression of TNN was intensely induced in hPDL transplants, while the expression level of SPON did not differ between cultured hPDL and hPDL transplants. Expression of both POSTN and COL12 was increased in hPDL transplants. Bar shows means ± SD (N=3). (B) Expression of tenascin-N and vimentin in hPDL cells of the transplant. Sections of hPDL cells of the transplant (a, c) and transplants without cells (HAP transplants) (b, d) were analyzed by *in situ* hybridization with tenascin-N, or by immunohistochemistory with human specific vimentin antibody (c, d). Expression of tenascin-N is seen in the hPDL cells of the transplant (a). No expression of tenascin-N is seen in the HAP transplants used as negative control (b). hPDL cells of the transplant are positive for human specific vimentin monoclonal antibody (c) however, HAP transplant is negative for anti-vimentin antibody (d). Bar: 100 μm.

by expression patterning with *in situ* hybridization analysis in mouse P1-DF and P35-PDL. As expected, the most abundantly expressed genes in the KK-Periome database were type I collagen and type III collagen, which are major fibrillar collagens in the PDL (Lukinmaa et al., 1993). Seven candidate genes with especially high expression in the PDL include SPARC, periostin, lumican, osteopontin, decorin, fibronectin and PLAP-1/Asporin (Takano-Yamamoto et al., 1994; Horiuchi et al., 1999; Yamada et al., 2001; Tenorio et al., 2003; Matheson et al., 2005). This expression profile was similar to the previous PDL-EST database (Yamada et al., 2001). Thus, the KK-Periome database reflects the PDL phenotype. In Table 3, 27 out of 39 EST clusters belonged to ECMs that are present in the PDL, providing additional evidence that the KK-Periome database represents the PDL phenotype. In the final step, we examined and compared the gene expression at the early stage of PDL formation (P1-DF) and the terminal differentiation stage (P35-PDL). F-spondin and tenascin-N were identified as candidate genes for early- and differentiation-stage markers, respectively. Periostin is a secreted adhesion protein that has homology with insect growth cone guidance protein fasciclin I (Horiuchi et al., 1999). During tooth germ development, periostin is expressed initially in the DF cells, and then restricted to postnatal PDL cells during the tooth root formation (Kruzynska-Frejtag et al., 2004). Periostin-deficient mice showed periodontal disease-like phenotype, suggesting a critical role of this protein in the maintenance of the PDL (Rios et al., 2005). Thus, periostin has been used as a marker for distinguishing PDL from adjacent connective tissues such as bone and gingiva in adult tissue (Saito et al., 2002; Yokoi et al., 2007). Although we were not investigating *periostin* splicing variant which is developmentally regulated by differential splicing (Kruzynska-Frejtag et al., 2004), *in situ* hybridization analysis and *in vivo* differentiation analysis revealed that expression of periostin could not distinguish adult PDL and DF cells. In contrast to periostin, F-spondin and tenascin-N were specifically expressed in DF and PDL respectively; furthermore *in vivo* differentiation analysis revealed that they are differentially expressed in PDL under *in vitro* and *in vivo* conditions. These findings strongly suggested that they might serve as PDL-lineage-specific markers.

4.2. F-spondin served as a marker for DF

The hypothesis that F-spondin is involved primarily in the initial process of PDL formation was further supported by our temporal and spatial expression analysis during tooth germ development. This is consistent with the notion that F-spondin may play a role in the early stage of PDL formation as demonstrated by the presence of high F-spondin mRNA level at E17 and P1-DF. Subsequently, F-spondin expression decreases dramatically at P35-PDL. In addition, *in vivo* differentiation assay revealed that F-spondin expression level did not change after implantation into SCID mice. Again, this is consistent with the idea that F-spondin may play a role in the early stage of PDL formation, especially those involved in PDL lineage. Although the precise function of F-spondin during tooth germ development is not yet clear, F-spondin expression was observed in P1 dermal papilla cells. Many ectodermal tissues such as teeth and hair share similar epithelial–mesenchymal interactions during early development (Pispa and Thesleff, 2003). Our data indicated that expression of F-spondin is detected at the site of epithelial–mesenchymal interaction in the dermal papilla (Supplementary Fig. 1, a and c), suggesting that signaling molecules involved in ectodermal organogenesis regulated the expression of F-spondin.

4.3. Expression of tenascin-N was induced in differentiated PDL

In the present study, we observed strong tenascin-N expression in the P35-PDL. Interestingly, tenascin-N expression was detected in P1-perichondrocyte of rib (Supplementary Fig. 1b and f) that forms ligament tissue, suggesting that tenascin-N may be associated with ligament tissue formation. In contrast to F-spondin, tenascin-N expression was restricted to the terminally differentiated PDL. To determine whether tenascin-N expression was regulated by PDL differentiation, we carried out an *in vivo* differentiation assay in which hPDL cell differentiation could be promoted by implantation into immunodeficient mouse (Saito et al., 2005). Interestingly, tenascin-N expression was significantly induced in hPDL cells upon implantation while no expression was observed in the *in vitro* cultured cells. This data suggested that hPDL cells express tenascin-N as a result of differentiation. Spatial and temporal expression analysis during PDL development coincided with the *in vivo* differentiation study, suggesting that tenascin-N could serve as a marker for differentiated PDL. Expression of tenascin-N was observed in periosteum at P1 mandible, but it was more strongly expressed in P35-PDL where tenascin-N expression was barely detectable in periosteum. These findings support that tenascin-N could serve as an adult PDL marker.

In summary, we established the KK-Periome database that provides a resource to identify genes involved in PDL development. We found that specific ECMs such as F-spondin and tenascin-N could serve as markers for DF and PDL, respectively, although more work is necessary to verify the actual function of these proteins/genes. Nevertheless, spatial and temporal expression analysis indicated that F-spondin and tenascin-N are related to the PDL differentiation process during the development of PDL lineage. Thus, the KK-Periome database might contain invaluable information regarding the transcripts (transcriptome) that are closely associated with human PDL formation.

Acknowledgements

We thank Dr. Toshio Kawase for providing hPDL cells and Dr. Eiro Kubota for help in obtaining human PDL samples. We are also grateful to Drs. Naohito Nozaki, Sachiko Iseki, Takamasa Yokoi and Takanori Tsubakimoto for their helpful advice and discussions during the course of this work. This work was supported by a Grant-in Aid for High-Tech Research Center Project from the Ministry of Education, Culture, Sports, Science and Technology of Japan (MEXT) the AGU High-Tech Research Center Project, the 2003 Multidisciplinary Research Project from MEXT, and grants from MEXT.

Appendix A. Supplementary data

Supplementary data associated with this article can be found, in the online version, at doi:10.1016/j.gene.2007.09.009.

References

D'Errico, J.A., MacNeil, R.L., Takata, T., Berry, J., Strayhorn, C., Somerman, M.J., 1997. Expression of bone associated markers by tooth root lining cells, in situ and in vitro. Bone 20, 117–126.

D'Errico, J.A., et al., 1999. Immortalized cementoblasts and periodontal ligament cells in culture. Bone 25, 39–47.

Hall, R.C., Embery, G., Lloyd, D., 1997. Immunochemical localization of the small leucine-rich proteoglycan in human predentine and dentine. Arch. Oral Biol. 42, 783–786.

Handa, K., et al., 2002. Cementum matrix formation in vivo by cultured dental follicle cells. Bone 31, 606–611.

Horiuchi, K., et al., 1999. Identification and characterization of a novel protein, periostin, with restricted expression to periosteum and periodontal ligament and increased expression by transforming growth factor beta. J. Bone Miner. Res. 14, 1239–1249.

Hou, L.T., et al., 1999. Characterization of dental follicle cells in developing mouse molar. Arch. Oral Biol. 44, 759–770.

Huang, X., Madan, A., 1999. CAP3: a DNA sequence assembly program. Genome Res. 9, 868–877.

Huang, Y.H., Ohsaki, Y., Kurisu, K., 1991. Distribution of type I and type III collagen in the developing periodontal ligament of mice. Matrix 11, 25–35.

Iseki, S., Wilkie, A.O., Heath, J.K., Ishimaru, T., Eto, K., Morriss-Kay, G.M., 1997. Fgfr2 and osteopontin domains in the developing skull vault are mutually exclusive and can be altered by locally applied FGF2. Development 124, 3375–3384.

Karimbux, N.Y., Rosenblum, N.D., Nishimura, I., 1992. Site-specific expression of collagen I and XII mRNAs in the rat periodontal ligament at two developmental stages. J. Dent. Res. 71, 1355–1362.

Kruzynska-Frejtag, A., et al., 2004. Periostin is expressed within the developing teeth at the sites of epithelial–mesenchymal interaction. Dev. Dyn. 229, 857–868.

Lukinmaa, P.L., Vaahtokari, A., Vainio, S., Sandberg, M., Waltimo, J., Thesleff, I., 1993. Transient expression of type III collagen by odontoblasts: developmental changes in the distribution of pro-alpha 1(III) and pro-alpha 1(I) collagen mRNAs in dental tissues. Matrix 13, 503–515.

Lukinmaa, P.L., Vaahtokari, A., Vainio, S., Thesleff, I., 1992. Expression of type I collagen pro-alpha 2 chain mRNA in adult human permanent teeth as revealed by in situ hybridization. J. Dent. Res. 71, 36–42.

Lukinmaa, P.L., Waltimo, J., 1992. Immunohistochemical localization of types I, V, and VI collagen in human permanent teeth and periodontal ligament. J. Dent. Res. 71, 391–397.

MacNeil, R.L., Berry, J.E., Strayhorn, C.L., Shigeyama, Y., Somerman, M.J., 1998. Expression of type I and XII collagen during development of the periodontal ligament in the mouse. Arch. Oral Biol. 43, 779–787.

Matheson, S., Larjava, H., Hakkinen, L., 2005. Distinctive localization and function for fibromodulin and decorin to regulate collagen fibril organization in periodontal tissues. J. Periodontal Res. 40, 312–324.

Matsuura, T., Duarte, W.R., Cheng, H., Uzawa, K., Yamauchi, M., 2001. Differential expression of decorin and biglycan genes during mouse tooth development. Matrix Biol. 20, 367–373.

McCulloch, C.A., 2006. Proteomics for the periodontium: current strategies and future promise. Periodontology 40, 173–183.

Petersson, U., Hultenby, K., Wendel, M., 2003. Identification, distribution and expression of osteoadherin during tooth formation. Eur. J. Oral Sci. 111, 128–136.

Pispa, J., Thesleff, I., 2003. Mechanisms of ectodermal organogenesis. Dev. Biol. 262, 195–205.

Rios, H., et al., 2005. Periostin null mice exhibit dwarfism, incisor enamel defects, and an early-onset periodontal disease-like phenotype. Mol. Cell Biol. 25, 11131–11144.

Sahlberg, C., Aukhil, I., Thesleff, I., 2001. Tenascin-C in developing mouse teeth: expression of splice variants and stimulation by TGFbeta and FGF. Eur. J. Oral Sci. 109, 114–124.

Saito, M., et al., 2005. Immortalization of cementoblast progenitor cells with Bmi-1 and TERT. J. Bone Miner. Res. 20, 50–57.

Saito, Y., et al., 2002. A cell line with characteristics of the periodontal ligament fibroblasts is negatively regulated for mineralization and Runx2/Cbfa1/Osf2 activity, part of which can be overcome by bone morphogenetic protein-2. J. Cell Sci. 115, 4191–4200.

Salmivirta, K., Sorokin, L.M., Ekblom, P., 1997. Differential expression of laminin alpha chains during murine tooth development. Dev. Dyn. 210, 206–215.

Sawada, T., et al., 2006. Immunohistochemical characterization of elastic system fibers in rat molar periodontal ligament. J. Histochem. Cytochem. 54, 1095–1103.

Seo, B.M., et al., 2004. Investigation of multipotent postnatal stem cells from human periodontal ligament. Lancet 364, 149–155.

Shibata, S., Yoneda, S., Yanagishita, M., Yamashita, Y., 2002. Developmental changes and regional differences in histochemical localization of hyaluronan and versican in postnatal molar dental pulp. Int. Endod. J. 35, 159–165.

Shibata, Y., Fujita, S., Takahashi, H., Yamaguchi, A., Koji, T., 2000. Assessment of decalcifying protocols for detection of specific RNA by non-radioactive in situ hybridization in calcified tissues. Histochem. Cell Biol. 113, 153–159.

Sloan, P., Carter, D.H., Kielty, C.M., Shuttleworth, C.A., 1993. An immunohistochemical study examining the role of collagen type VI in the rodent periodontal ligament. Histochem. J. 25, 523–530.

Takano-Yamamoto, T., Takemura, T., Kitamura, Y., Nomura, S., 1994. Site-specific expression of mRNAs for osteonectin, osteocalcin, and osteopontin revealed by in situ hybridization in rat periodontal ligament during physiological tooth movement. J. Histochem. Cytochem. 42, 885–896.

Ten Cate, A.R. (Ed.), 1994. Oral Histology, Development, Structure, and Function. Mosby, St. Louis.

Tenorio, D.M., Santos, M.F., Zorn, T.M., 2003. Distribution of biglycan and decorin in rat dental tissue. Braz. J. Med. Biol. Res. 36, 1061–1065.

Tsubota, M., Sasano, Y., Takahashi, I., Kagayama, M., Shimauchi, H., 2002. Expression of MMP-8 and MMP-13 mRNAs in rat periodontium during tooth eruption. J. Dent. Res. 81, 673–678.

Venter, J.C., Levy, S., Stockwell, T., Remington, K., Halpern, A., 2003. Massive parallelism, randomness and genomic advances. Nat. Genet. 33, 219–227.

Wilkinson, D.G., 1995. RNA detection using non-radioactive in situ hybridization. Curr. Opin. Biotechnol. 6, 20–23.

Worapamorn, W., Li, H., Pujic, Z., Xiao, Y., Young, W.G., Bartold, P.M., 2000. Expression and distribution of cell-surface proteoglycans in the normal Lewis rat molar periodontium. J. Periodontol. Res. 35, 214–224.

Yamada, S., et al., 2001. Expression profile of active genes in human periodontal ligament and isolation of PLAP-1, a novel SLRP family gene. Gene 275, 279–286.

Yokoi, T., et al., 2007. Establishment of immortalized dental follicle cells for generating periodontal ligament in vivo. Cell Tissue Res. 327, 301–311.